

1

Supplementary Material

2 **Divergent impacts of antibiotics on ferrihydrite biotransformation by**
3 ***Shewanella oneidensis*: electron transfer regulation and iron redox**
4 **cycling**

5 Xinyue Li^{1†}, Jianxin Chen^{1†}, Xiyuan Chen¹, Yuxin Wang¹, Jieyu Li¹, Xiangchun Guo¹, Yan Shi^{1,2},
6 Kejing Zhang^{1,2*}, Zhang Lin^{1,2}

7 ¹*School of Metallurgy and Environment, Central South University, Changsha 410083, China*

8 ²*Chinese National Engineering Research Center for Control & Treatment of Heavy Metal*
9 *Pollution, Changsha 410083, China*

10 *Corresponding author. Email: 22022126@csu.edu.cn

11 †These authors contributed equally to this work.

12 Number of pages: 26 (including cover page)

13 Number of tables: 6

14 Number of figures: 13

15

16 **Content summary**

17 **Supplementary materials and methods**

18 **Table S1.** The concentrations of antibiotics used in this study.

19 **Table S2.** Specific primer sequences for quantitative real-time PCR analysis of Mtr pathway-
20 associated genes in MR-1.

21 **Table S3.** Mössbauer hyperfine parameters of spectra from Figure 2 measured at room
22 temperature.

23 **Table S4.** Fe(II) concentrations at 5 h for each treatment group in Figure 4a and significance
24 analysis.

25 **Table S5.** The fluorescence intensities of peaks in 3D-EEM of EPS fractions excreted by MR-1
26 incubated with SMX and CAP at 5 h of incubation.

27 **Table S6.** The pseudo-first-order kinetic consumption rates of SMX and CAP.

28 **Figure S1.** Morphology and particle size distribution of synthesized Fh. (a) SEM image and particle
29 size histogram derived from SEM; (b) particle size distribution determined by dynamic light
30 scattering.

31 **Figure S2.** Biomass of MR-1 incubated with PCG. CK-neg1: MR-1 cultured without sodium
32 lactate; CK-neg2: heat-killed MR-1 cells cultured with sodium lactate. The treatment with PCG did
33 not affect the biomass of MR-1.

34 **Figure S3.** Total Fe(II) production of Fh incubated with SMX or CAP. Fe(II) production of Fh
35 induced by SMX or CAP alone was negligible.

36 **Figure S4.** XRD spectra of the solids from cultures incubated for 5 h with the addition of various
37 antibiotics. The dashed lines correspond to the positions of the characteristic peaks of goethite.

38 **Figure S5.** SEM images of solids in cultures incubated for one month with SMX and CAP added.

39 **Figure S6.** SAED pattern of solids from the biotransformation of Fh with CAP after one month of
40 incubation. The dashed lines correspond to the positions of the characteristic crystal planes of
41 goethite and magnetite, respectively.

42 **Figure S7.** Biomass of MR-1 incubated with SMX or CAP. CK-neg1: MR-1 cultured without
43 sodium lactate; CK-neg2: heat-killed MR-1 cells cultured with sodium lactate. Treatments with
44 SMX or CAP did not affect the biomass of MR-1.

45 **Figure S8.** XRD patterns of solids from Fh incubated with SMX or CAP for one month. Neither
46 SMX nor CAP is capable of catalyzing the conversion of Fh to magnetite or goethite.

47 **Figure S9.** Total Fe(II) production from Fh pre-equilibrated with antibiotics and subsequently
48 reduced by MR-1.

49 **Figure S10.** XRD spectra of solids from the one-month biotransformation of Fh pre-
50 equilibrated with antibiotics.

51 **Figure S11.** Transformation products of CAP (a) and SMX (b) after 10 h of incubation with Fh

52 and MR-1.

53 **Figure S12.** XRD spectra of solids from Fh transformation catalyzed by exogenous aqueous
54 Fe(II), with and without the addition of SMX, following one-month incubation.

55 **Figure S13.** SEM image and EDS mapping of the solids formed from Fe(II) incubated with
56 SMX after 5 h of incubation.

57 **References**

58

59 **Supplementary materials and methods**

60 **Text S1**

61 **Sources of chemicals.** LB broth was purchased from Sangon Biotech. MOPs and $\text{FeCl}_3 \cdot 6\text{H}_2\text{O}$
62 were purchased from Aladdin at 99.0% purity and analytical grade, respectively. Penicillin G
63 Sodium (PCG) was purchased from Solarbio at 95% purity. Lincomycin (LCM), acetonitrile, and
64 methanol were all purchased from Sigma-Aldrich at 99.5%, 99.9%, and 99.9% purity, respectively.
65 Other reagents used (e.g. NaCl, L-sodium lactate, sodium fumarate, sulfamethoxazole (SMX),
66 ciprofloxacin (CIP), erythromycin (ERY), tetracycline (TC), and chloramphenicol (CAP), etc.)
67 were all purchased from Macklin at analytical grade. All solutions were prepared using Milli-Q
68 ultrapure water. Furthermore, to facilitate the dissolution process, hydrochloric acid and acetic acid
69 were added to dissolve SMX and CIP, respectively. Ethanol served as the solubilizing agent for
70 ERY, TC, and CAP.

71 **Text S2**

72 **Synthesis of ferrihydrite (Fh).** Fh was synthesized by following a previous study.¹ In brief, a
73 solution of 0.4 M $\text{FeCl}_3 \cdot 6\text{H}_2\text{O}$ was mixed with a 1 M NaOH solution on a magnetic stirrer for a
74 duration of 3 h, until the pH reached a range of 7.0 to 8.0. Subsequently, the suspension was allowed
75 to react for an additional 6 h. To purify the suspension, ultrapure water was added to remove the
76 supernatant, and this process was repeated at least 5 times until the residual chloride concentration
77 was reduced to below 1 mM. The resultant purified Fh slurry was resuspended in ultrapure water
78 and stored in a refrigerator at 4°C until needed. The concentrations of Fe(III) and Fe(II) ions were
79 then determined using a spectrophotometric method, as described in a later section. The scanning
80 electron microscopy (SEM, MIRA3 LMH, Czech Republic) and particle size analyzer (Brookhaven
81 Instruments Co, NanoBrook Omni, USA) were used to characterize the particle size distribution of
82 synthesized Fh.

83 **Text S3**

84 **Measurement of Fe(II) concentration.** To characterize the reduction degree of Fh, a modified
85 *o*-phenanthroline spectrophotometric method was adopted to quantify Fe(II) concentration.²
86 Initially, 2 mL of the suspension was collected and completely dissolved in 6 M hydrochloric acid
87 (HCl). A specific volume of the aforementioned acidized solution was mixed into 0.5 mL of acetate
88 buffer (prepared by dissolving 400 g of ammonium acetate and 500 mL of ice acetic acid per liter,
89 adjust to pH 4.5). Subsequently, 0.2 mL of 0.5 wt% *o*-phenanthroline solution was added, and the
90 mixture solution was diluted with ultrapure water to a final volume of 5 mL. The absorbance was
91 measured at 510 nm by UV-vis UV-1780 spectrophotometers, after chromogenic reaction for 15
92 min. To determine the total iron (Fe_{total}) concentration, aliquots of the aforementioned acidized
93 solution were mixed with 1 mL of 10 wt% hydroxylamine hydrochloride solution to fully reduce
94 Fe(III) ions to Fe(II) ions. The total Fe(II) concentration (equal to Fe_{total}) was then determined using
95 the *o*-phenanthroline spectrophotometric method. Subsequently, the Fe(III) concentration was
96 calculated by subtracting the Fe(II) concentration from the Fe_{total} concentration.

97 **Text S4**

98 **Determination of concentrations and byproducts for SMX and CAP.** At each sampling
99 time, 2 mL of the suspensions were collected from the incubations and filtered through a 0.22 μm
100 nylon filter. Subsequently, the filtrate samples were filtered using a sodium type cation exchange
101 resin filter (IC-Na 1cc) to remove iron, after which the concentrations of SMX and CAP, along with
102 product determination, were conducted. Concentrations of SMX and CAP were measured using
103 ultra performance liquid chromatography with photo-diode array detection (UPLC-PDA;
104 ACQUITY H-class).^{3, 4} The stationary phase was a ACQUITY UPLC® BEH C18 (1.7 μm , 2.1
105 mm \times 50 mm). The mobile phase flowed at a rate of 0.1 mL min⁻¹, with an injection volume of 10
106 μL . SMX and CAP were detected at wavelengths of 268 nm and 278 nm, respectively. For SMX
107 concentration analysis, an isocratic mobile phase composed of 80% aqueous buffer (20 mM
108 phosphate buffer adjusted to pH 3.0) and 20% acetonitrile (v/v) was used. In addition, CAP
109 concentration analysis utilized a mobile phase containing 40% water (0.1% formic acid) and 60%
110 methyl alcohol (v/v).

111 Furthermore, the degradation products of SMX and CAP were determined using a liquid
112 chromatography system (Agilent 1290uplc) coupled with a quadrupole time-of-flight mass
113 spectrometer (Agilent qtof6550), equipped with an electrospray ion (ESI) source.^{3, 4} The stationary
114 phase for this analysis was ACQUITY UPLC® BEH C18 (1.7 μm , 2.1 mm \times 100 mm). The mobile
115 phase flowed at a rate of 0.3 mL min⁻¹, with a sample size of 5 μL . To test the byproducts of SMX,
116 mobile phases A (0.1% formic acid) and B (acetonitrile) were used. The elution gradient began with
117 100% phase A for 4 min, followed by a transition to 90% phase A and 10% phase B within 2 min.
118 Then, it was converted to 60% of phase A and 35% of phase B within 4 min, kept for 3 min, and
119 finally switched back to 100% phase A within 1 min, which was maintained for 1 min. For CAP
120 byproducts, mobile phases A (0.1% formic acid) and B (methanol) were used, with a 50% elution
121 ratio of phase A and 50% phase B, retention time of 15 min. The mass charge ratio (m/z) of MS
122 analysis was 50~1000, with a sheath temperature of 350°C, a sheath gas flow of 12 L min⁻¹, a voltage
123 of 4000 V in ESI⁺ mode, and 3200 V in ESI-mode.

124 **Text S5**

125 **Extraction of extracellular polymeric substance (EPS).** The heating method was used
126 according to a previously reported procedure.⁵ Initially, 20 mL of the reaction suspension
127 (containing cells) was collected and washed with PBS (0.1 M, pH=7.0). Subsequently, the cells
128 were dispersed in 10 mL of 0.05% (wt%) NaCl solution. The suspension was then heated in a water
129 bath for 30 min at 70°C, centrifuged at 8000 g for 15 min, and the supernatant was regarded as the
130 extracted EPS.

131 **Text S6**

132 **Electrochemical analyses.** Differential pulse voltammetry (DPV) was performed by an
133 electrochemical workstation (Multi Autolab M204, Metrohm, Switzerland).⁶ A conventional quartz
134 three-electrode electrochemical cell was used for all electrochemical experiments with glassy

135 carbon electrode (GCE), platinum wire, and Ag/AgCl (sat. KCl) as working, counter, and reference
136 electrodes, respectively. For the determination of the extracellular electron transfer type of MR-1,
137 5 μ L of bacterial droplets, washed twice with PBS (100 mM, pH=7.0), were absorbed onto the
138 surface of the GCE. After drying, 2 μ L 5% Nafion dispersion was applied to form a film on the
139 surface. The electrolyte, containing 30 mM MOPS (pH=7.0) and 25 mM KCl, was deaerated by
140 bubbling with N₂ for more than 45 min. The DPV parameters were set as follows: E_i = -0.6 V; E_f =
141 0.4 V; amplitude, 60 mV; pulse width, 200 ms; and potential increment, 6 mV.

142 **Tables**

143 **Table S1.** The concentrations of antibiotics used in this study.

Antibiotic species	Working concentration (µg/mL)	Antibiotic concentration per unit of bacteria in this system (µg/cells)	Environmental concentration (µg/kg) ^{7, 8}		Location	Antibiotic concentration per unit of bacteria in environment (µg/cells)
			min	max		
SMX	100.00	2×10^{-6}	1.80	6207.60	Animal farm manure	2.00×10^{-12} - 8.87×10^{-3}
CIP	100.00	2×10^{-6}	1.50	10111.10	Animal farm manure	1.67×10^{-12} - 1.44×10^{-2}
ERY	100.00	2×10^{-6}	4.20	91.00	Animal farm manure	4.67×10^{-12} - 1.30×10^{-4}
PCG	100.00	2×10^{-6}	0.01	974.00	sediment	1.11×10^{-14} - 1.39×10^{-3}
TC	50.00	1×10^{-6}	4.50	9260.00	Animal farm manure	5.00×10^{-12} - 1.32×10^{-2}
LCM	50.00	1×10^{-6}	164.00	17000.00	Animal farm manure	1.82×10^{-10} - 2.43×10^{-2}
CAP	25.00	5×10^{-7}	42.20	42.20	Animal farm manure	4.69×10^{-11} - 6.03×10^{-5}

144 Given that in natural environments, there are 10^3 ~ 10^7 microorganisms in 1 g of soil,⁹ and soil bacteria account for 70%~90% of the total number of soil
 145 microorganisms, the bacteria count in the environment can be estimated to be the range of 7×10^2 to 9×10^8 cells g⁻¹.

146 **Table S2.** Specific primer sequences for quantitative real-time PCR analysis of Mtr pathway-
 147 associated genes in MR-1.

Gene ID	Description	Primers
	16sDNA	Forward sequence (5'-3'): CCCTGGACAAAGACTGACGC Reverse sequence (5'-3'): AGACACCAAACCTCCGAGTAGACA
SO_RS08155	OmcA	Forward sequence (5'-3'): AAGGTGGCGAGCGTCATAC Reverse sequence (5'-3'): CACAATCTGCGGCTGGTTT
SO_RS21330	CymA	Forward sequence (5'-3'): GATTGGTGTGTGGGCTATTTT Reverse sequence (5'-3'): GATGCCAGCACTTCATTCTTC
SO_RS08145	Mtr A	Forward sequence (5'-3'): CGTATGTCTTGGAATGGCG Reverse sequence (5'-3'): TGAGTGGGTGACTTGAGCGT
SO_RS08140	Mtr B	Forward sequence (5'-3'): TTA CTGGCAACCGCCTTCT Reverse sequence (5'-3'): CTGCACCGACCACATCTACC
SO_RS08150	Mtr C	Forward sequence (5'-3'): CGATTTTGCTGCGGGTAA Reverse sequence (5'-3'): TGAACACTAATTGTGGCTGCTT
SO_1782	Mtr D	Forward sequence (5'-3'): ATCCCAACATCAAAGATTCCC Reverse sequence (5'-3'): GTTGCCTTTCCAAGCGATAC
SO_1781	Mtr E	Forward sequence (5'-3'): CGGACTTACCCACGTTTCTTA Reverse sequence (5'-3'): TACTGCCCGCTTGATCTGA
SO_1780	Mtr F	Forward sequence (5'-3'): AAGCATCAGCAGTGCCAGTAT Reverse sequence (5'-3'): GTTCCCCAGTTAGCATAAATCC

148

149 **Table S3.** Mössbauer hyperfine parameters of spectra from Figure 2 measured at room temperature.

Sample	Attribution	δ (mm/s)	Δ or ϵ (mm/s)	HF (T)	RA (%)
Initial Fh substrates					
Fh	Fh	0.27	0.75	—	100
Biotic transformation products in 5 h					
CK	Goethite	0.27	0.51	—	10.5
	Fh	0.26	0.79	—	89.5
SMX added	Goethite	0.24	0.52	—	24.7
	Fh	0.24	0.84	—	75.3
CAP added	Goethite	0.27	0.53	—	24.0
	Fh	0.26	0.85	—	76.0
Biotic transformation products in 1 month					
CK	Magnetite (tetra)	0.11	-0.19	48.38	38.4
	Magnetite (octa)	0.63	0.25	47.68	33.7
	Goethite	0.34	-0.07	31.40	21.2
	Fh	0.34	2.28	—	6.7
SMX added	Magnetite (tetra)	0.04	-0.26	48.33	38.6
	Magnetite (octa)	0.51	0.23	47.74	36.3
	Goethite	0.02	0.25	29.68	18.3
	Fh	0.39	2.09	—	6.7
CAP added	Magnetite (tetra)	0.19	-0.21	49.46	2.8
	Magnetite (octa)	0.43	0.21	46.76	16.2
	Goethite	0.24	-0.08	30.38	54.6
	Fh	0.23	0.76	—	26.4

150 δ , isomer shift taking α -iron as reference at room temperature; Δ or ϵ , quadrupole splitting; HF,
 151 hyperfine magnetic field; RA, relative abundance; tetra, tetrahedral site; octa, octahedral site.

152 **Table S4.** Fe(II) concentrations at 5 h for each treatment group in Figure 4a and significance
 153 analysis.

Treatment group	Fe(II) concentration (mM)	Significance vs. CK	Significance vs. Corresponding Direct Treatment Group
CK	0.81 ± 0.07	-	-
MR-1 + SMX + Fh	1.70 ± 0.04	P < 0.01 (**)	-
pre-equilibrated MR-1 + SMX	1.00 ± 0.13	P > 0.05 (ns)	P < 0.01 (**) (vs. MR-1 + SMX + Fh)
MR-1 + CAP + Fh	0.36 ± 0.06	P < 0.01 (**)	-
pre-equilibrated MR-1 + CAP	0.31 ± 0.02	P < 0.01 (**)	P > 0.05 (ns) (vs. MR-1 + CAP + Fh)

154 All data are expressed as mean ± standard deviation. Statistical analysis was performed using one-
 155 way ANOVA followed by a pairwise test. Significance levels are marked as follows: **P < 0.01
 156 (extremely significant difference), *P < 0.05 (significant difference), ns (no significant difference,
 157 P > 0.05).

158 **Table S5.** The fluorescence intensities of peaks in 3D-EEM of EPS fractions excreted by MR-1
159 incubated with SMX and CAP at 5 h of incubation.

	Peak A		Peak B		Peak C	
	Ex/Em (nm)	Intensity (AU)	Ex/Em (nm)	Intensity (AU)	Ex/Em (nm)	Intensity (AU)
CK	285/335	46.38	365/445	48.13	445/520	90.79
SMX	290/340	77.87	360/450	47.17	445/520	87.95
CAP	290/340	28.19	-	-	445/520	75.78

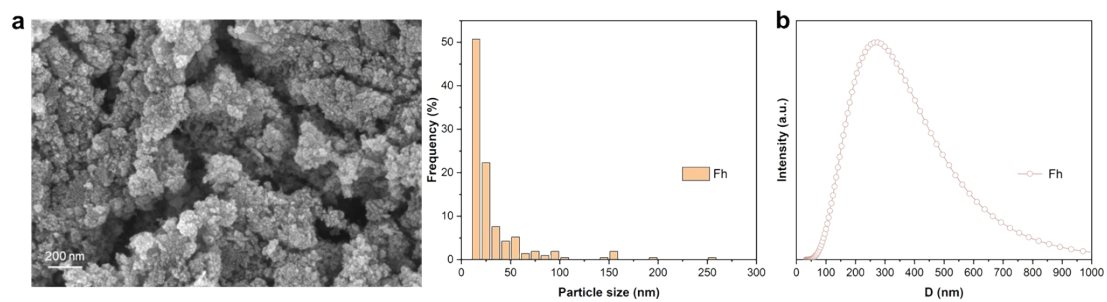
160

161 **Table S6.** The pseudo-first-order kinetic consumption rates of SMX and CAP.

	Pseudo-first-order kinetic consumption rates of antibiotics (h^{-1})		
	antibiotic + MR-1	antibiotic + Fh	antibiotic + MR-1 + Fh
SMX	0.001	0.001	1.41
CAP	0.063	0.0008	0.91

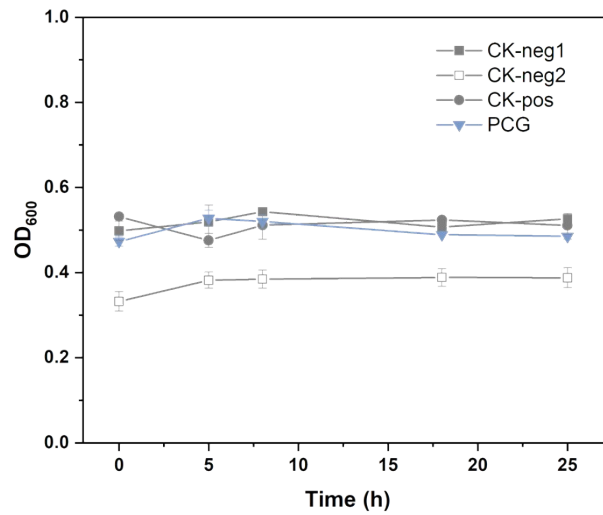
162

163 **Figures**



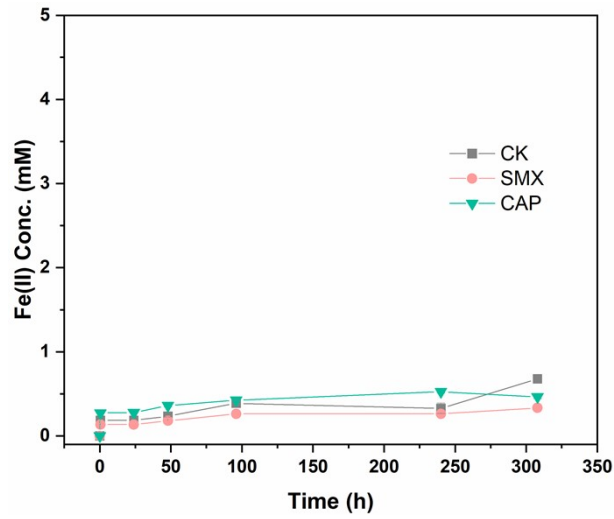
164

165 **Figure S1.** Morphology and particle size distribution of synthesized Fh. (a) SEM image and particle
166 size histogram derived from SEM; (b) particle size distribution determined by dynamic light
167 scattering.



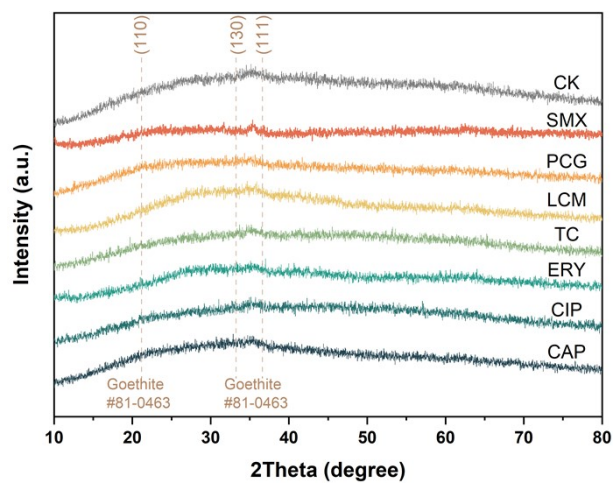
168

169 **Figure S2.** Biomass of MR-1 incubated with PCG. CK-neg1: MR-1 cultured without sodium
 170 lactate; CK-neg2: heat-killed MR-1 cells cultured with sodium lactate. The treatment with PCG did
 171 not affect the biomass of MR-1.



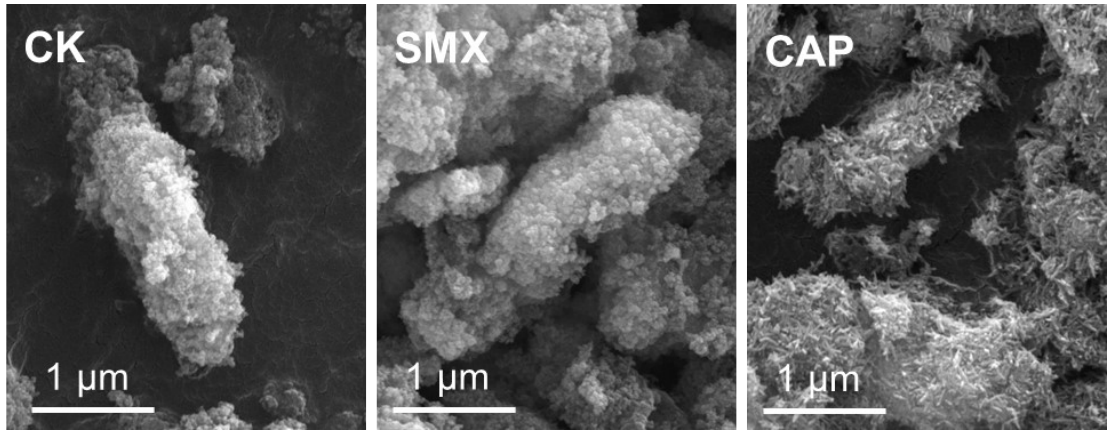
172

173 **Figure S3.** Total Fe(II) production of Fh incubated with SMX or CAP. Fe(II) production of Fh
174 induced by SMX or CAP alone was negligible.



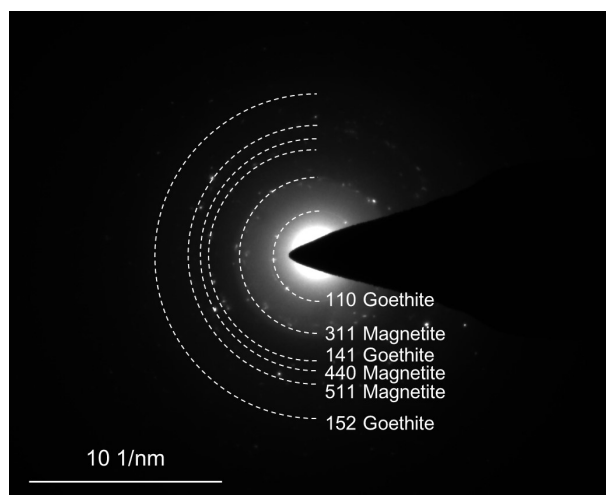
175

176 **Figure S4.** XRD spectra of the solids from cultures incubated for 5 h with the addition of various
177 antibiotics. The dashed lines correspond to the positions of the characteristic peaks of goethite.



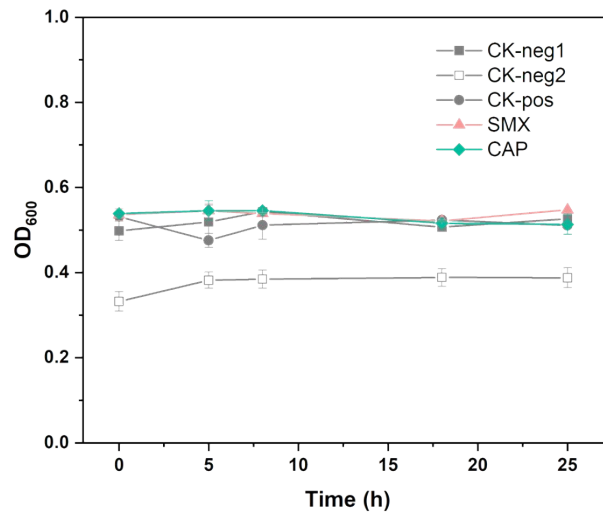
178

179 **Figure S5.** SEM images of solids in cultures incubated for one month with SMX and CAP added.



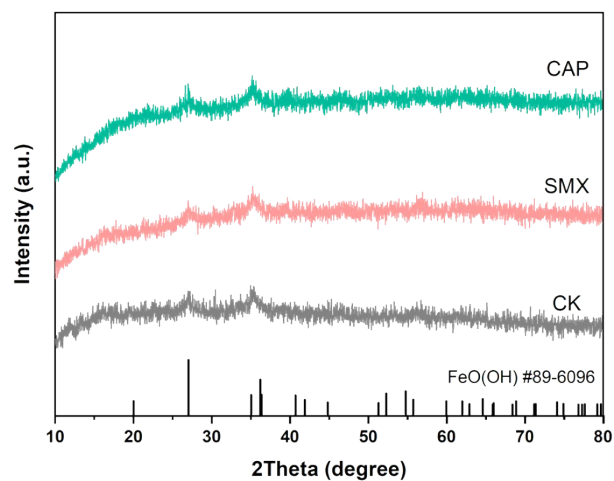
180

181 **Figure S6.** SAED pattern of solids from the biotransformation of Fh with CAP after one month of
182 incubation. The dashed lines correspond to the positions of the characteristic crystal planes of
183 goethite and magnetite, respectively.



184

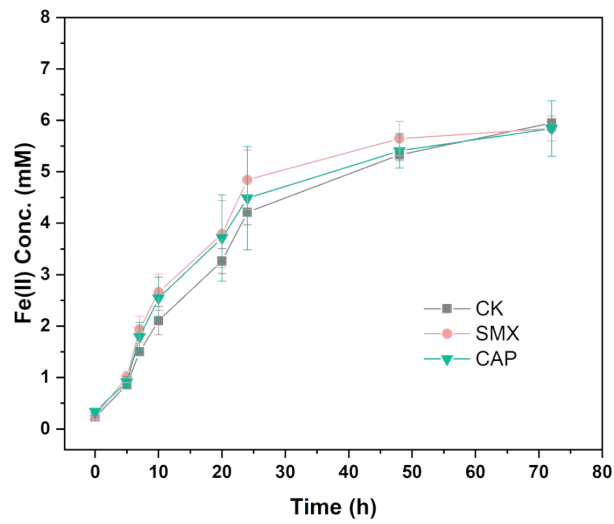
185 **Figure S7.** Biomass of MR-1 incubated with SMX or CAP. CK-neg1: MR-1 cultured without
 186 sodium lactate; CK-neg2: heat-killed MR-1 cells cultured with sodium lactate. Treatments with
 187 SMX or CAP did not affect the biomass of MR-1.



188

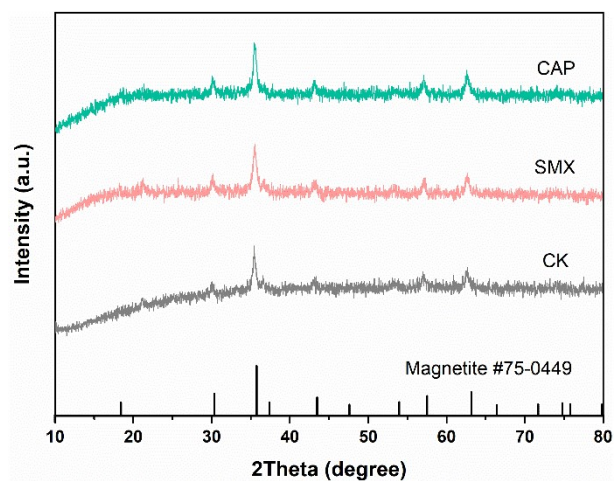
189 **Figure S8.** XRD patterns of solids from Fh incubated with SMX or CAP for one month. Neither

190 SMX nor CAP is capable of catalyzing the conversion of Fh to magnetite or goethite.



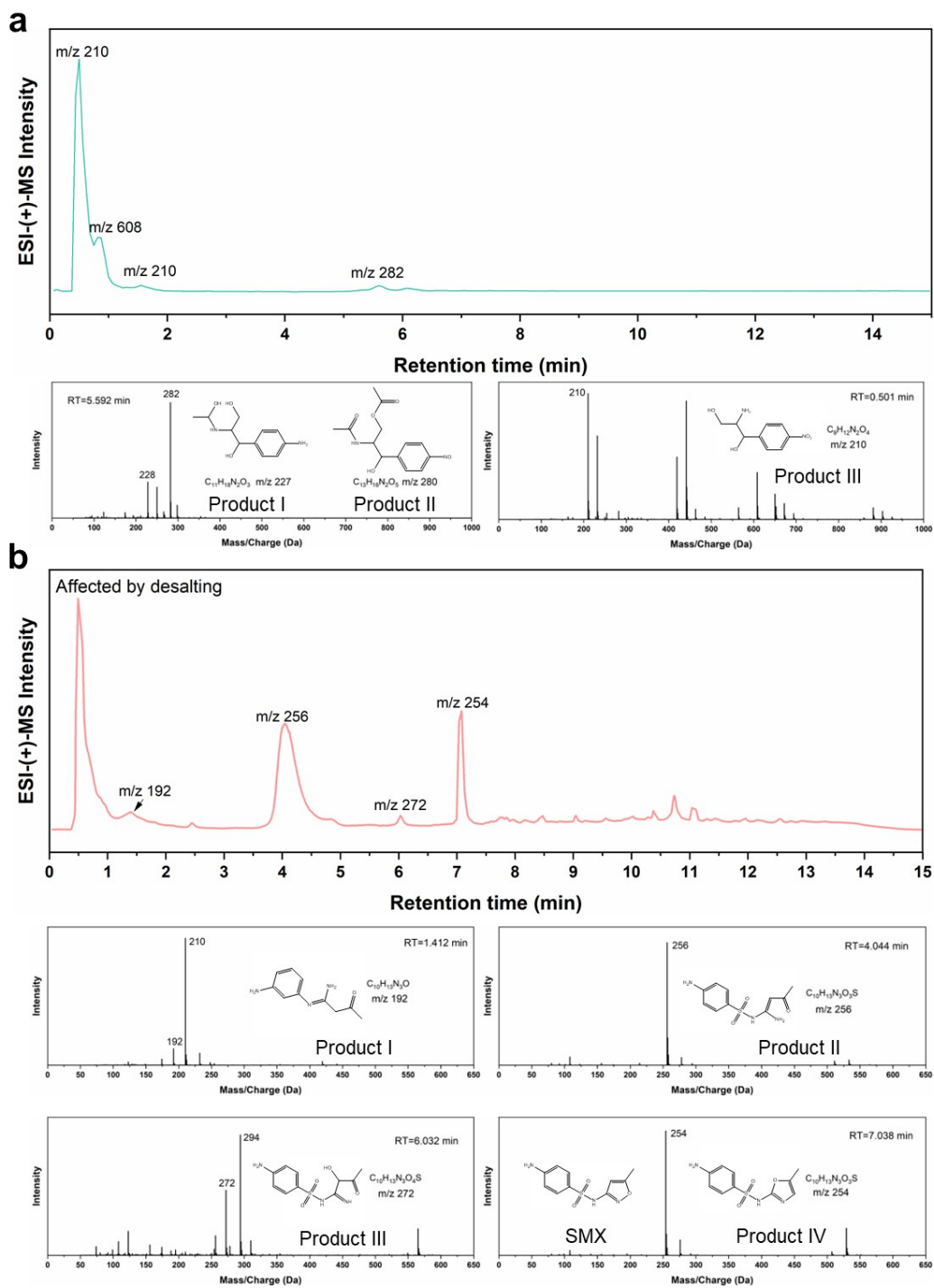
191

192 **Figure S9.** Total Fe(II) production from Fh pre-equilibrated with antibiotics and subsequently
193 reduced by MR-1.



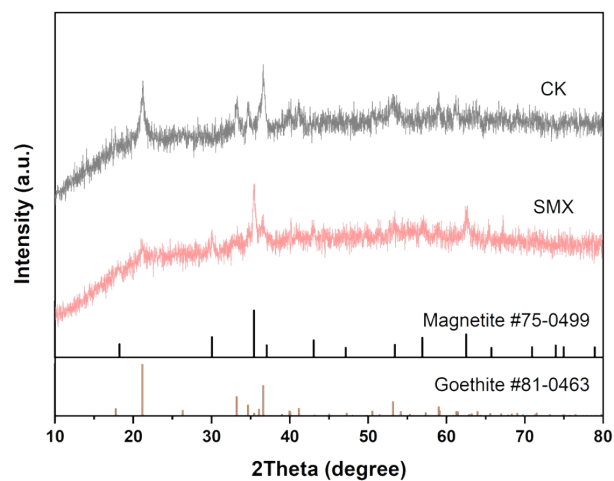
194

195 **Figure S10.** XRD spectra of solids from the one-month biotransformation of Fh pre-equilibrated
196 with antibiotics.



198

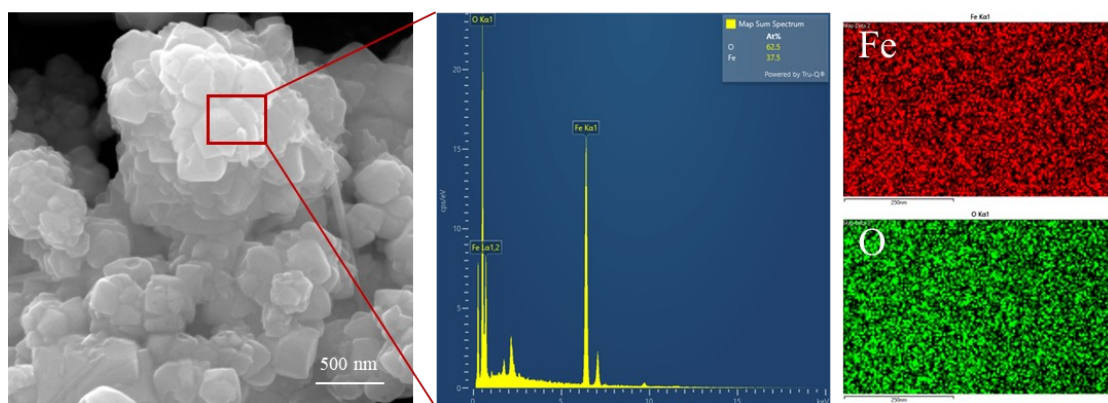
199 **Figure S11.** Transformation products of CAP (a) and SMX (b) after 10 h of incubation with Fh
 200 and MR-1.



201

202 **Figure S12.** XRD spectra of solids from Fh transformation catalyzed by exogenous aqueous Fe(II),

203 with and without the addition of SMX, following one-month incubation.



204
 205 **Figure S13.** SEM image and EDS mapping of the solids formed from Fe(II) incubated with SMX
 206 after 5 h of incubation.

207 References

208

209 1. U. Schwertmann and R. M. Cornell, *Iron oxides in the laboratory: preparation and*
210 *characterization*, John Wiley & Sons, 2008.

211 2. F. Zhu, Y. Huang, H. Ni, J. Tang, Q. Zhu, Z.-e. Long and L. Zou, Biogenic iron sulfide
212 functioning as electron-mediating interface to accelerate dissimilatory ferrihydrite reduction by
213 *Shewanella oneidensis* MR-1, *Chemosphere*, 2022, **288**, 132661.

214 3. J. L. Mohatt, L. Hu, K. T. Finneran and T. J. Strathmann, Microbially mediated abiotic
215 transformation of the antimicrobial agent sulfamethoxazole under iron-reducing soil conditions,
216 *Environ. Sci. Technol.*, 2011, **45**, 4793-4801.

217 4. D. Wu, S. Huang, X. Zhang, H. Ren, X. Jin and C. Gu, Iron minerals mediated interfacial
218 hydrolysis of chloramphenicol antibiotic under limited moisture conditions, *Environ. Sci.*
219 *Technol.*, 2021, **55**, 9569-9578.

220 5. W. Yan, W. Guo, L. Wang and C. Jing, Extracellular polymeric substances from *Shewanella*
221 *oneidensis* MR-1 biofilms mediate the transformation of ferrihydrite, *Sci. Total Environ.*, 2021,
222 **784**, 147245.

223 6. Y. Xiao, E. Zhang, J. Zhang, Y. Dai, Z. Yang, H. E. Christensen, J. Ulstrup and F. Zhao,
224 Extracellular polymeric substances are transient media for microbial extracellular electron
225 transfer, *Sci. Adv.*, 2017, **3**, e1700623.

226 7. F. Huang, Z. An, M. J. Moran and F. Liu, Recognition of typical antibiotic residues in
227 environmental media related to groundwater in China (2009–2019), *J. Hazard. Mater.*, 2020,
228 **399**, 122813.

229 8. C. Chemtai, F. O. Kengara and A. N. Ngigi, Levels and ecological risk of pharmaceuticals in
230 River Sosiani, Kenya, *Environ. Monit. Assess.*, 2023, **195**, 431.

231 9. D. Yu and J. Li, *Wei sheng wu xue [Microbiology]*, Science Press, 2nd edn., 1985.

232